I&EC research
Industrial & Engineering Chemistry Research

pubs.acs.org/IECR

Article

DFT Studies on Thermal and Oxidative Degradation of Monoethanolamine

Christopher Parks,* Ehsan Alborzi, Muhammad Akram, and Mohammed Pourkashanian

Cite This: https://dx.doi.org/10.1021/acs.iecr.0c03003

Read Online

ACCESS | Metrics & More | Article Recommendations | Supporting Information

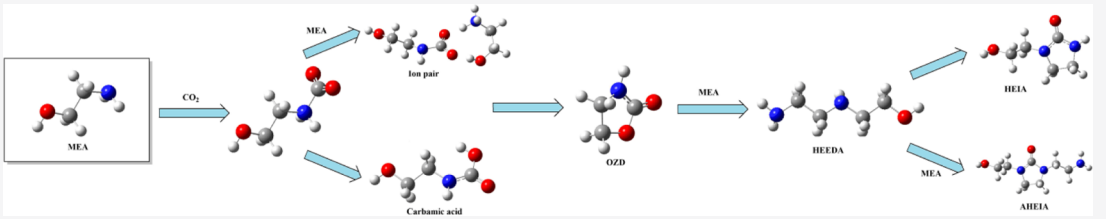

ABSTRACT: Thermal and oxidative degradation of monoethanolamine (MEA) represents a major problem for modern day carbon capture technologies. Here, we report on a series of density functional theory (DFT) calculations investigating the possible chemical pathways leading to the formation of the most commonly observed degradation products. 2-Oxyzolidinone (OZD) can be formed from ring closure reactions of carbamates, carbamic acids, or isocyanates. The latter, itself, formed by dehydration of MEA. *N*-(2-hydroxethyl)ethylenediamine (HEEDA), 1-(2-hydroxyethyl)imidazolidone (HEIA), and *N*-(2-aminoethyl)-*N*′-(2-hydroxyethyl)-imidazolidin-2-one (AHEIA) are all hypothesized to form favorably from degradation reactions of OZD. MEA can undergo oxidative degradation to form imines and hydroperoxides. This work details the mechanistic steps leading to the formation of these species that could help in the location of new compounds that aim to prevent their formation in future systems. Moreover, the thermochemical data will aid in the construction of a chemical kinetic mechanism to rationalize the rate of formation of all the species in real systems.

1. INTRODUCTION

At the Conference of the United Nations Framework Convention on Climate Change (UNFCCC) in December 2015, representatives of 195 nations adopted the Paris Climate Agreement.[1] The agreement pledges a response to the threat posed by global climate change and aims to keep the global temperature rise in the 21st century well below 2 °C above the preindustrial levels. Further efforts are to be made to limit the temperature increase even further to below 1.5 °C. To aid in achieving this goal, the global peak for greenhouse gas (GHG) emissions should be reached imminently. Efforts are to be made in establishing a carbon-neutral global society and economy in the second half of the 21st century. This can only be achieved through significant contributions of all sectors that currently generate GHG emissions. In some sectors, particularly aviation and agriculture, GHG emissions will be difficult to eliminate entirely. Thus, technologies are required to compensate the effects of such emissions by removing the gases from the atmosphere.

One such methodology aiming to achieve this is carbon capture and utilization (CCU). These technologies consist of CO_2 capture and conversion technologies, as well as those for hydrogen production. However, despite the potential environmental advantages these technologies offer, the uptake and deployment of CCU presents a number of technical and economic challenges. Such challenges are driving current scientific progress and research. It is noteworthy that there remains an ambiguity as to the extent climate change benefits from deployment of CCU systems. These depend on several factors including the kind of technology used, the type of conversion product manufactured, the source and nature of the energy needed to power such conversion, the source of the CO_2 feedstock, and the location and characteristics of the CCU installation.[2]

One of the technical challenges associated with CCU technologies is the instability of chemical medium used for the carbon capture stage, in particular, the use of aqueous amine-based solutions. These solutions are able to absorb CO_2 from flue gas after combustion. To date, monoethanolamine (MEA) is the most widely studied and understood chemical for this process. It has the advantages of being highly water soluble, has good absorption kinetics, low volatility, and high CO_2 loading at favorable temperatures.[3] However, this technology currently does not see widespread use as it is hindered by costs

Received: June 16, 2020
Revised: July 31, 2020
Accepted: August 3, 2020
Published: August 3, 2020

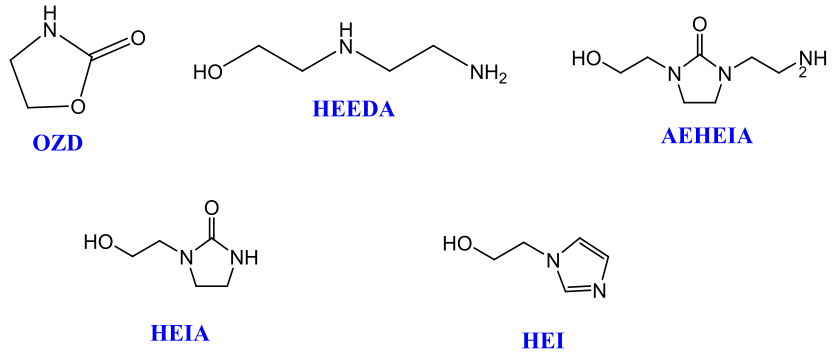

Figure 1. Major thermal degradation products of MEA.

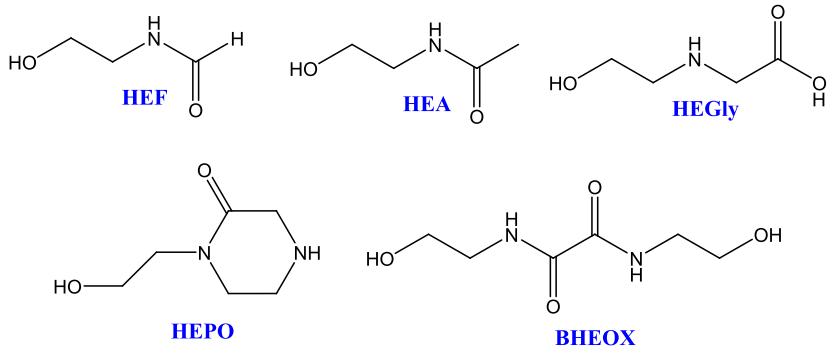

Figure 2. Selected oxidative degradation products of MEA.

associated with solvent degradation and regeneration. The cost of solvent regeneration is reported to be as high as 10% of the total cost of CO_2 capture.[4−6] Moreover, the degradation products are often corrosive and are hazardous to the environment.

The thermal degradation of MEA has been studied experimentally since the 1950s.[7,8] The chemical reactions occur mainly in the stripper in experimental plants and are believed to be accelerated by higher temperatures, pressures, and higher concentrations of CO_2. It is hypothesized that the first step of thermal degradation proceeds through the cyclization of carbamates and carbonic acids resulting in the formation of 2-oxazolidinone (OZD). This is an intermediate species and rapidly reacts to form other degradation products. Research in this field has identified *N*-(2-hydroxethyl)-ethylenediamine (HEEDA), 1-(2-hydroxyethyl)imidazolidone (HEIA), *N*-(2-aminoethyl)-*N*′-(2-hydroxyethyl)imidazolidin-2-one (AHEIA), and *N*-(2-hydroxyethyl)imidazole (HEI) as some of the most common degradation products.[9] The molecular structures of these species are shown in Figure 1.

A number of different mechanisms have been proposed to explain not only the formation of these species but also the order in which they are formed. Kim et al. proposed mechanisms for the degradation of diethanolamine (DEA),[10] which has since been expanded on by Davis et al. for MEA degradation.[9]

Oxidative degradation of MEA is less well understood than thermal degradation, though the mechanism is considered to be driven by radicals.[11,12] It generally occurs in the absorber, where the amount of dissolved oxygen and CO_2 is relatively high compared to the stripper. The observed products are generally categorized into two sets of compounds: primary and secondary. Primary products such as aldehydes, carboxylic acids, alcohols, and ammonia are directly formed from MEA. The exact nature of the mechanism is still unclear, but it is likely initiated by abstraction of a hydrogen radical from either the nitrogen atom or the α-carbon or β-carbon. Which one of these abstractions dominates is dependent on a combination of the molecular structure of the amine, pH, solvent environment, and nature of the oxidant.

Secondary products are formed either from the primary degradation products in isolation or through the reaction of primary species of oxidative degradation with the amine. Some examples of these species include *N*-(2-hydroxyethyl)-formamide (HEF), *N*-(2-hydroxyethyl)-acetamide (HEA), *N*,*N*′-bis(2-hydroxyethyl)-oxamide (BHEOX), *N*-(2-hydroxyethyl)piperazin-2-one (HEPO), and *N*-(2-hydroxyethyl)glycine (HEGLY). They are illustrated in Figure 2.

To date, there have also been a few computational studies on the degradation of amines in publicly available literature. Vevelsted et al. calculated the free energies of formation of some of the most common degradation products.[13] Saeed et al. reported on the formation of imidazolidine species.[14] Yoon et al. more recently reported AIMD simulations looking into the elementary reactions of thermal degradation of amines. They found that the formation of OZD, HEEDA, and HEIA is all thermodynamically favorable.[15] Davran-Candan modeled the CO_2 capture step using various amines and found that carbamates were the dominating products for MEA systems.[16] A number of other papers focussed on studying the carbon capture step by amines.[16−19]

A robust theoretical framework, if thoroughly validated and sufficiently detailed, would allow for the prediction and control of thermal degradation of MEA so that carbon capture operation units can be designed to have an acceptable maintenance frequency and life span. The present paper describes computational studies looking into deducing the

https://dx.doi.org/10.1021/acs.iecr.0c03003
Ind. Eng. Chem. Res. XXXX, XXX, XXX−XXX

chemical pathways leading to the formation of major degradation species formed from MEA. Whilst a particular focus is placed on the mechanisms leading to product formation arising from thermal decomposition, oxidative degradation is also investigated. Mechanisms rationalizing the formation of OZD, HEEDA, HEIA, AHEIA, BHEU, and HEPO are presented. It is hoped that such data will form the basis of a full chemical kinetic model that aims to predict the formation and depreciation of the key species in the process as a function of time.

2. COMPUTATIONAL DETAILS

All calculations in the paper were performed on Gaussian 09, revision D.01.[20] The B3LYP functional[21−23] and cc-PVTZ[24] basis set were used throughout this study. This functional has been shown to be suitable for studying aqueous MEA systems previously in the literature.[15,25,26] Equivalent calculations to those reported here using the M06 functional[27] and Def2TZVP basis set can be found in the Supporting Information. Solvent effects were accounted for using the default polarizable continuum model (PCM) as implemented in Gaussian 09.[28] The solvent parameters for water were used in each case.[29] Results for equivalent calculations to those reported in the main text using the SMD solvent model[30] can be found in the Supporting Information. An ultrafine grid and empirical dispersion corrections through the GD3 keyword were applied to all calculations.[31] Optimized structures were confirmed as local minima by the absence of imaginary frequencies. Transition states were confirmed both by the presence of one large negative frequency corresponding to the expected saddle point and with intrinsic reaction coordinate scans (IRCs). Transition states were optimized using the QST3 method as implemented in Gaussian.[32] Free energies were calculated using the Grimme quasiharmonic entropy correction using the GoodVibes script.[33]

3. RESULTS AND DISCUSSION

3.1. Carbamate and Carbonic Acid Formation. According to Davis and Rochelle, the major products of thermal degradation of MEA, as identified by chromatography, in descending order are HEIA, AHEIA, HEEDA, and OZD.[9] OZD is generally considered as an intermediate species, both because it is observed in small quantities and mechanistic pathways can be envisaged where it can react to form the other product species mentioned above.[9]

A thorough investigation into the initial formation of carbamate, carbamic acid, and bicarbonate species is not necessary here, having already received a great deal of literature attention.[19,34−38] The exact nature of the CO_2 absorption step is still under debate, with the existence of an intermediate zwitterion species still a controversial topic. Iida and co-workers[39] and Arstad et al.[40] each found a stable zwitterion in an aqueous solution. More recently, Xie et al. performed more accurate calculations using CCSD(T) and found a reaction mechanism where the formation of a zwitterion is the rate determining step.[41]

Here, our first consideration was the formation of carbamate and carbamic acid for comparison with existing literature data. The nitrogen atom of MEA can act as a nucleophile and react with dissolved CO_2 in the solution to form a carbamate. The generated carbamate can subsequently undergo a hydrogen transfer reaction either intramolecularly (though a 1,3 H-transfer reaction) or facilitated through transfer to, and from, a further molecule of MEA or H_2O to form carbamic acid. Moreover, the carbamate could exist as an ion pair with a protonated MEA molecule. The energy profiles for these processes are summarized in Figure 3.

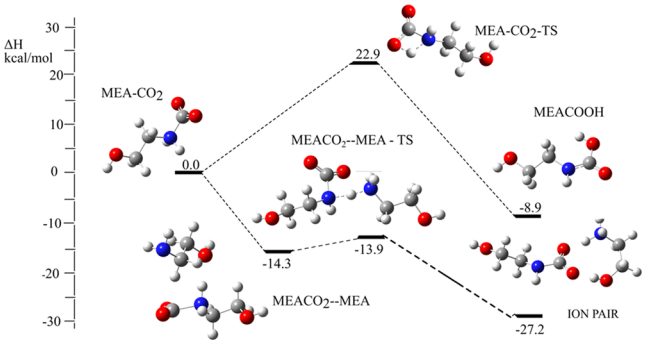

Figure 3. Density functional theory (DFT)-calculated ΔH energy profile for the proposed formation of either carbamic acid or an ion pair from MEA-CO_2 (carbamate species).

Both product species, the carbamate or the ion pair, are formed via a H-transfer reaction to either the carboxylate oxygen or nitrogen atom of a neighboring MEA molecule, respectively. Given that nitrogen atoms are more basic than oxygen atoms, it is of no surprise that the formation of an ion pair has both a lower activation energy (0.4 cf. 22.9 kcal mol^{-1}) and a more favorable reaction enthalpy compared to carbamic acid formation (−27.2 cf. −8.9 kcal mol^{-1}). However, the formation of carbamic acid could become significant at higher CO_2 loadings where the concentration of MEA-CO_2 would far exceed that of free MEA and thus favor formation of carbamic acid.

3.2. OZD Formation from Carbamates, Carbamic Acid, and Isocyanates. Next, the cyclization of the product species to form OZD was investigated. Given that the formation of an ion pair is more favorable than carbamic acid, this was used as a starting point for further optimization. The energy profile for formation of OZD is shown in Figure 4.

In the transition state, the carboxylate oxygen attacks the carbon atom, α, to the hydroxyl group, thus forming a five-membered ring. Concurrently, the hydroxide leaving group abstracts a proton from the nearby ammonium cation ultimately forming OZD, water, and regenerating MEA. The activation energy for this reaction is 39.5 kcal mol^{-1}, and the

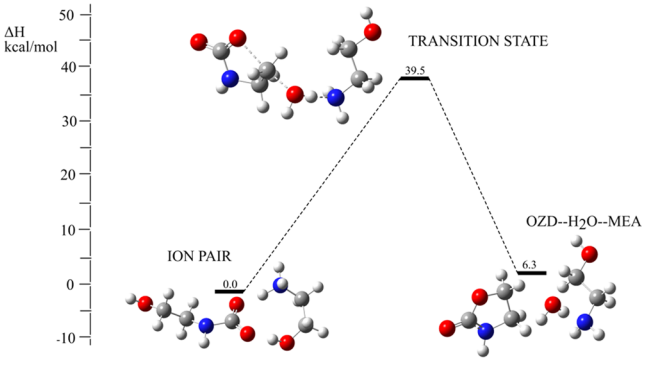

Figure 4. DFT-calculated ΔH energy profile for the proposed formation of OZD from an ion pair.

https://dx.doi.org/10.1021/acs.iecr.0c03003
Ind. Eng. Chem. Res. XXXX, XXX, XXX−XXX

Scheme 1. OZD Formation via Dehydration of Carbamic Acid and Subsequent Cyclization of the Product

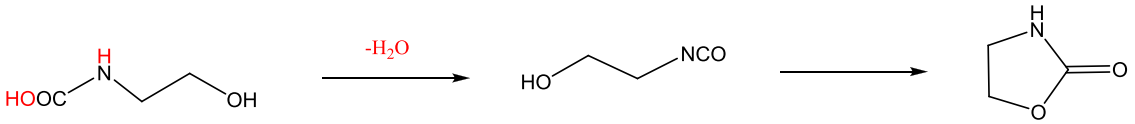

overall reaction is endoergic by 6.3 kcal mol^{-1}. Whilst the activation energy is appreciably high, it is still permissible under standard experimental conditions generally observed in the stripper.

Another possible route to formation of OZD is via cyclization of isocyanates, as shown in Scheme 1. Such species have been reported to form from the dehydration of carbamic acids.[42,43]

Two distinct transition states leading to the dehydration of carbamic acid were located. The first involved intramolecular dehydration whereby the N−H hydrogen reacts with the hydroxyl motif of the carboxylic acid group to liberate water and isocyanate. The second involved two concurrent hydrogen transfer reactions facilitated by an explicit water molecule in the calculation (shown in Figure 5). The intramolecular

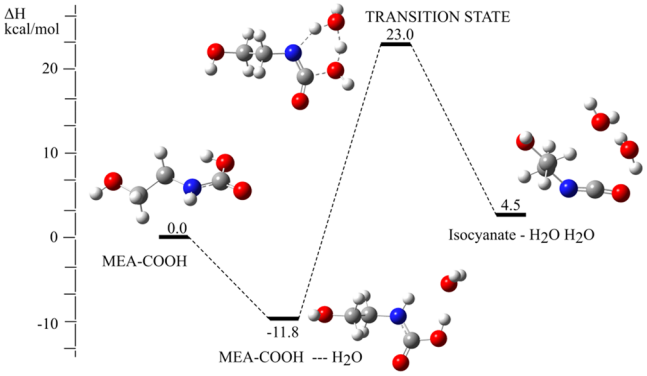

Figure 5. DFT-calculated ΔH energy profile for the proposed formation of isocyanate from carbamic acid, facilitated by a nearby water molecule.

reaction had an activation energy of 47.0 compared with 34.8 kcal mol^{-1} for the water-facilitated reaction. Given that the reaction medium has significant quantities of water, this route will be preferred. The overall reaction is endoergic with a reaction energy of +4.5 kcal mol^{-1}. The generated isocyanate can then go on to react further. Two potential species that might form and thus investigated here are cyclization leading to the formation of OZD and reaction with a further molecule of MEA to form BHEU.[3]

The formation of BHEU, a related compound to UREA, is presented in Scheme 2, and the energy profile is shown in Figure 6. In the transition state, the nitrogen atom on MEA acts as a nucleophile and reacts with the electrophilic carbon atom of the isocyanate molecule. At the same time, a hydrogen atom is transferred from the $-NH_2$ group to the nitrogen atom on the isocyanate group. This reaction has an activation energy

Scheme 2. Possible Route to BHEU Formation via Reaction of MEA and Isocyanate

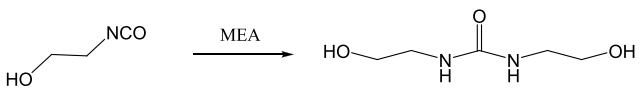

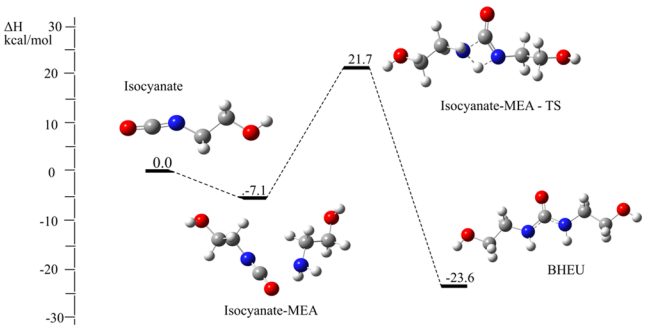

Figure 6. DFT-calculated ΔH energy profile for the proposed formation of BHEU from the reaction of isocyanate and MEA.

of 28.7 kcal mol^{-1} and a reaction energy of −23.6 kcal mol^{-1}. Given the large excess of MEA present in the stripper and the relatively low reaction barrier, it is likely that any isocyanate that does form does not accumulate and can rapidly react further to form BHEU.

The second reaction of isocyanate investigated was cyclization to form OZD. Transition states could not be located for cyclization from either protonated or neutral isocyanate. Scan calculations suggested that there was no barrier to either reaction. However, a transition state for the reaction was found to be facilitated by the addition of both a protonated and a neutral MEA molecule. The energy profile is shown in Figure 7. In the transition state, the neutral MEA acts as a base and accepts a proton from the hydroxyl group of the isocyanate. The oxygen then reacts with the carbonyl carbon, and the forming ring accepts a proton from the protonated MEA molecule. The activation energy is 2.9 kcal mol^{-1}, which is very low and suggests a facile reaction. The reaction energy is −35.3 kcal mol^{-1}. Similar values were reported by Yoon et al.[15]

3.3. HEEDA Formation. High performance liquid chromatography (HPLC) investigations undertaken independently by Davis and Lepaumier identified that HEEDA is formed prior to the formation of HEIA or AHEIA but is observed after the formation of OZD.[9,44] Hence, the formation of HEEDA was investigated next. It is believed to form via a ring opening reaction between OZD and MEA in accordance with Scheme 3.[45]

In this reaction, the nitrogen atom on the MEA molecule acts as a nucleophile and attacks OZD. This causes the ring to open by breaking the C−O bond. Subsequent hydrogen transfer can occur either facilitated through transfer to and from a molecule of either water or MEA or intramolecularly through a 1,4 H-transfer. This is accompanied by loss of CO_2, which ultimately generates HEEDA. The energy profile is shown in Figure 8.

The activation energy for the initial attack of MEA on OZD is 27.2 kcal mol^{-1}. This forms an intermediate zwitterion species, which can undergo an internal hydrogen transfer reaction to form a species that can more readily release the bound CO_2 molecule. This reaction is predicted to have a very

https://dx.doi.org/10.1021/acs.iecr.0c03003
Ind. Eng. Chem. Res. XXXX, XXX, XXX−XXX

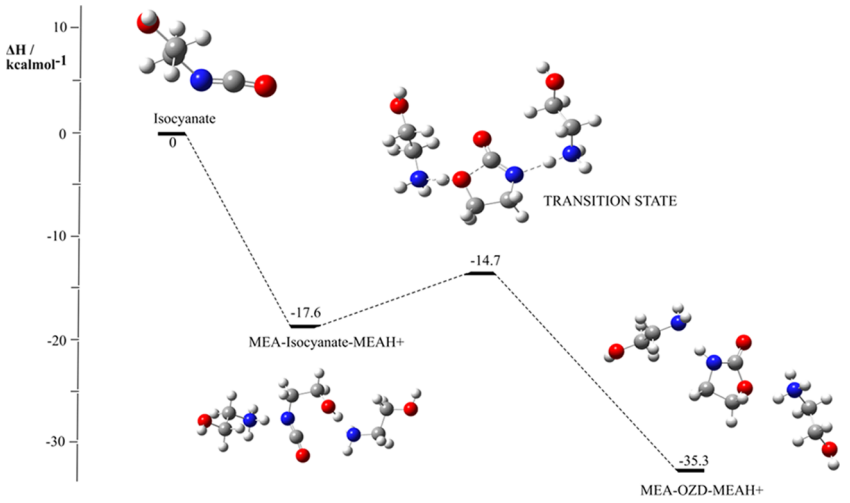

Figure 7. DFT-calculated ΔH energy profile for the proposed formation of OZD from isocyanate, facilitated by MEA and protonated MEA.

Scheme 3. HEEDA Formation from OZD and MEA

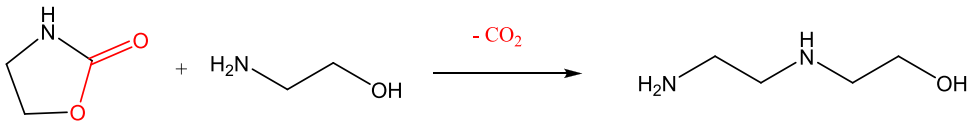

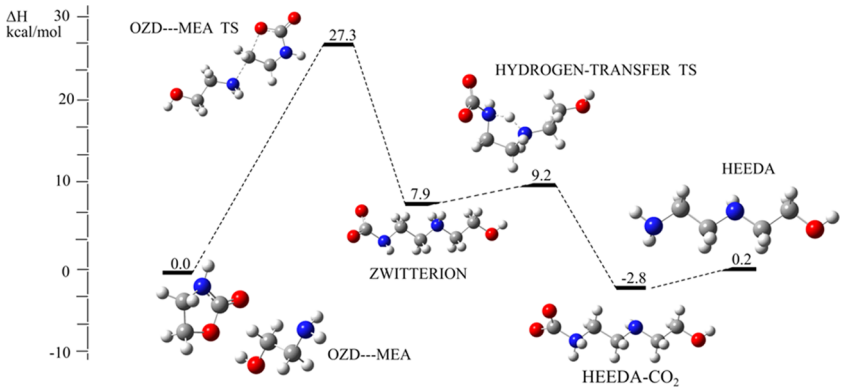

Figure 8. DFT-calculated ΔH energy profile for the proposed formation of HEEDA from OZD and MEA.

low activation energy of 1.3 kcal mol^{-1} and is typical for intramolecular reactions, which are generally faster than intermolecular reactions. Overall, the reaction to form HEEDA from OZD and MEA is very slightly endoergic with a predicted reaction energy of 0.2 kcal mol^{-1}. Given the standard operating conditions for these reactions, the formation is still more than feasible.

3.4. HEIA and AHEIA Formation. Data accrued from both NMR studies and HPLC analysis has shown that HEIA is the most observed product species arising from thermal degradation of MEA.[9] One route to its formation is through the reaction of HEEDA and CO_2, as shown in Scheme 4.

Figure 9 shows the energy profile for HEIA formation. There are two nitrogen atoms on the HEEDA molecule either of which could react with CO_2 to form the initial carbamate species. It was found that reaction at the terminal nitrogen atom was less favorable, most likely due to the lower basicity of the primary compared to the secondary nitrogen atom. The carbamate species can then undergo a 1,3 H-transfer reaction transferring a hydrogen from the nitrogen to the carboxylate oxygen to form carbamic acid. This was also observed in the reaction of MEA and CO_2.

The carbamic acid species formed as a result of this hydrogen transfer is marginally less stable than the separated reactants (+2.7 kcal mol^{-1}). However, it can undergo a cyclization reaction that is concurrent with the elimination of water to form HEIA. The transition state for this reaction is shown in Figure 10. The terminal nitrogen atom acts as a nucleophile and attacks the electrophilic carbon atom on the carboxylic acid group.

The overall reaction energy for the formation of HEIA is −6.7 kcal mol^{-1}. This is consistent with experimental observations that suggest that this species is observed in higher concentrations compared to other products.

Scheme 4. HEIA Formation from HEEDA

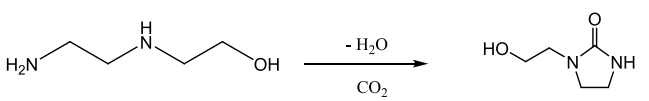

https://dx.doi.org/10.1021/acs.iecr.0c03003
Ind. Eng. Chem. Res. XXXX, XXX, XXX−XXX

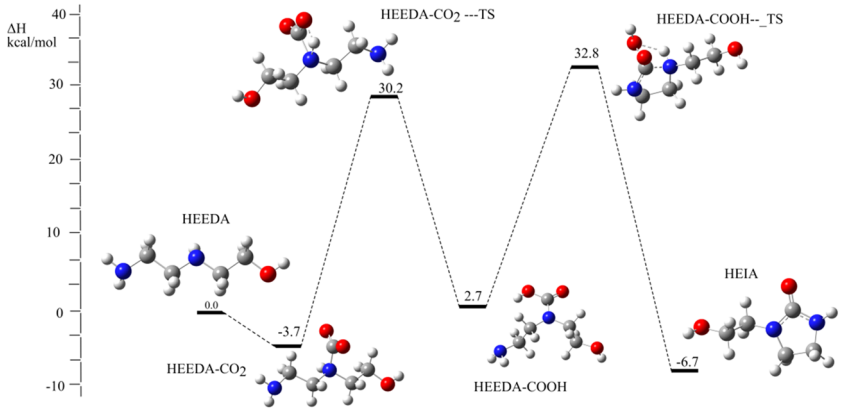

Figure 9. DFT-calculated ΔH energy profile for the proposed formation of HEIA from HEEDA.

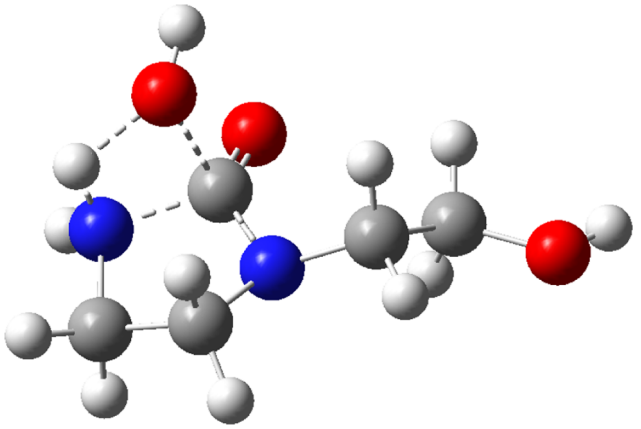

Figure 10. DFT-optimized transition state structure for the cyclization reaction leading to the formation of HEIA.

AHEIA is formed in a related reaction to that for HEIA, as shown in Scheme 5. The energy profile is shown in Figure 11. Either the terminal nitrogen or the secondary nitrogen atom can act as a nucleophile and attack an electrophilic carbon atom on a molecule of OZD. This causes the OZD ring to open with an activation energy of 26.6 kcal mol^{-1}. Subsequent hydrogen transfer (activation energy 33.7 kcal mol^{-1}) and cyclization (activation energy 30.7 kcal mol^{-1}) lead to the formation of AHEIA.

The overall reaction energy is −10.9 kcal mol^{-1}. This is comparable to the calculated value for the formation of HEIA. It is likely that AHEIA is observed in smaller amounts due to the low concentrations of OZD, which is necessary for its formation. In contrast, AHEAI needs only a further molecule of MEA, which is in great excess. This is consistent with experimental observations where more AHEIA is formed than HEIA.

3.5. Oxidative Degradation of MEA. *3.5.1. MEA Radical, Peroxide, and Imine formation.* Oxidative degradation is generally considered to occur in the presence of oxygen from flue gas.[46,47] Furthermore, trace metal ions such as Fe^{2+}, Cr^{3+}, Ni^{2+}, and Mn^{2+} are also believed to play an important role. However, whilst the exact mechanism of oxidative degradation still remains unclear, it is considered to be initiated by electron and/or hydrogen abstraction from the amine.[12,48] These radicals could originate from metals, from dissolved oxygen, or via the presence of alkyl radicals.[49,50] The reported products from oxidative degeneration are vast. They include but are not limited to ammonia, formaldehyde, ethanol, glyoxal, oxalic acid, methylamine, formamide, glycol, glycine, acetone, and imidazolidine.

Figure 12 shows the DFT-calculated energy profile for abstraction of hydrogen radicals from four positions on MEA. To reduce the computational cost of the calculations, an ethyl radical was chosen as a model for $R^{\bullet}$. The activation energies for the abstractions ranged from 8.2 to 10.8 kcal mol^{-1}. The most stable product resulted from abstraction of a hydrogen radical from the carbon α to the amino group. However, abstraction at either carbon or the nitrogen results in an exoergic reaction leading to stable products.

The radical species formed here is often reported to react with oxygen and through subsequent proton abstraction and elimination forms an imine and hydrogen peroxide as shown in Scheme 6. The DFT-calculated energy profile is shown in Figure 13.

The initial binding of oxygen to the MEA-radical species unsurprisingly is favorable. The following step where the peroxy radical species, $H_2NCH(OO^{\bullet})CH_2OH$, picks up a hydrogen radical, most likely from water or another molecule of MEA, is also highly favored. This forms a peroxide species, $H_2NCH(OOH)CH_2OH$. Despite multiple attempts, a transition state whereby HOOH is eliminated from this species in isolation could not be located. To address this, an explicit water molecule was included in the calculations, which acted to facilitate the elimination reaction. Given the large excess of water in the experimental system, this is a reasonable approach. The transition state is shown in Figure 14.

In the transition state, a hydrogen atom is transferred from the water molecule to the −OOH group forming hydrogen peroxide. Concurrently, a hydrogen is transferred from the nitrogen on the MEA radical to the −OH group, which acts to reform the water molecule. The activation energy for this

Scheme 5. AHEIA Formation from OZD and HEEDA

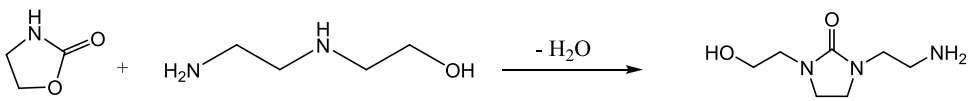

https://dx.doi.org/10.1021/acs.iecr.0c03003
Ind. Eng. Chem. Res. XXXX, XXX, XXX−XXX

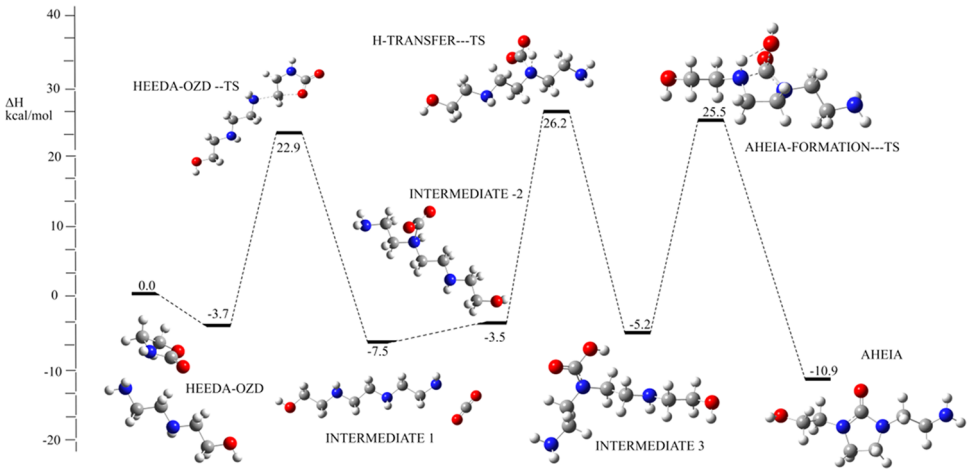

Figure 11. DFT-calculated ΔH energy profile for the proposed formation of AHEIA.

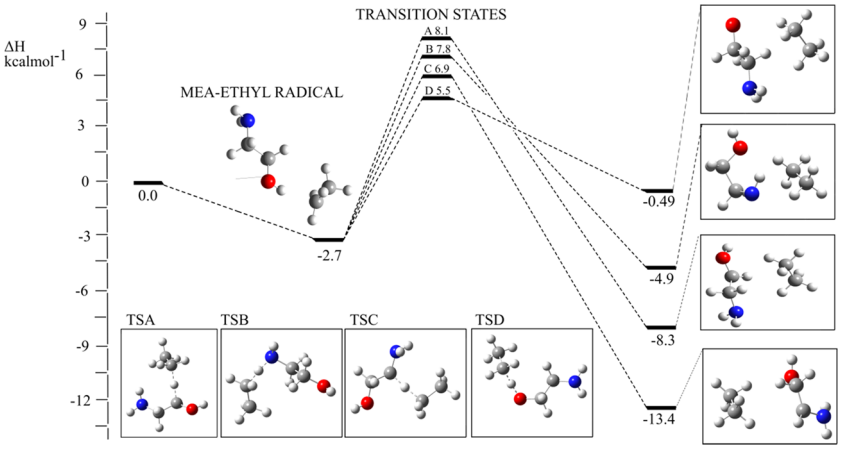

Figure 12. DFT-calculated ΔH energy profile for the hydrogen radical abstraction from four sites on MEA by an ethyl radical.

Scheme 6. Proposed Formation of an Imine and Hydrogen Peroxide from MEA

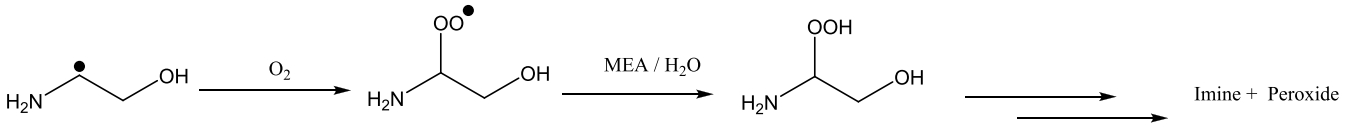

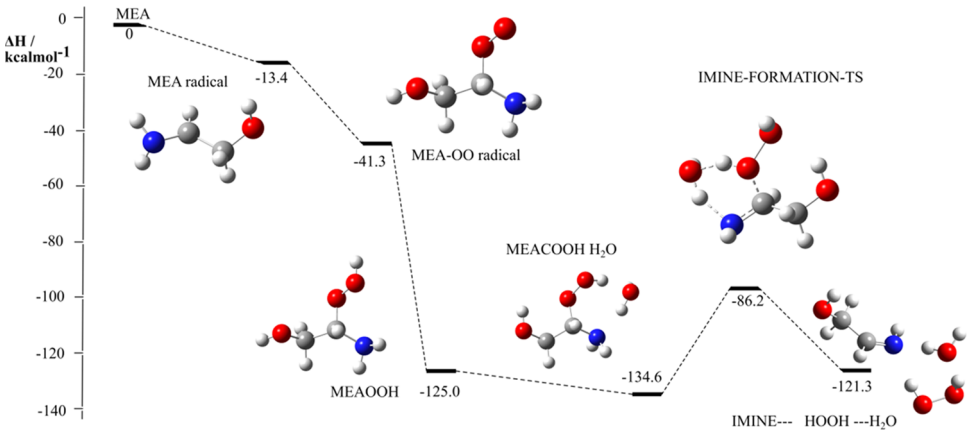

Figure 13. DFT-calculated ΔH energy profile for the formation of an imine and HOOH from MEA.

transfer is 48.4 kcal mol^{-1}, which is high and potentially prohibitive even at the elevated temperatures and pressures experienced in the experiments. The reaction is also endoergic (13.3 kcal mol^{-1}). The transition state could potentially be

https://dx.doi.org/10.1021/acs.iecr.0c03003
Ind. Eng. Chem. Res. XXXX, XXX, XXX−XXX

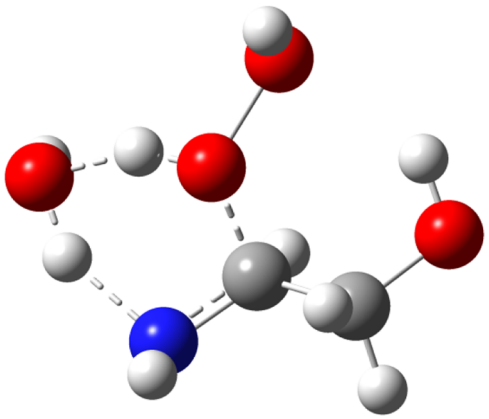

Figure 14. DFT-calculated transition state for the formation of HOOH, H_2O, and an imine from $H_2NCH(OOH)CH_2OH$.

stabilized by further interactions with more water molecules, or it could be that there is another route to formation of the imine. The former was investigated next.

The precollision complex, transition state, and product complex were all reoptimized with an additional explicit water molecule to investigate whether this made this chemical pathway more feasible. A comparison of the energy profiles for reactions containing one and two water molecules is shown in Figure 15. This additional water molecule acts to lower the activation energy from 48.4 to 28.7 kcal mol^{-1}. The product complex was also further stabilized with two water molecules as opposed to one. It is clear to see that additional water molecules increase the kinetic and thermodynamic viability of imine formation from the peroxide species.

3.5.2. Reaction between MEA and Organic Acids. A number of studies have shown that amide species can form in pilot plants from oxidative degradation.[3,44,47,51,52] These species can be formed from the reaction of MEA and organic acids, as shown in Scheme 7.

The energy profile for the formation of HEF from the condensation reaction of MEA and formic acid is shown in Figure 16. This reaction is initiated by nucleophilic attack of the nitrogen atom of MEA on the carbonyl carbon of formic acid. Several H-transfer reactions afford the product complex and water. This is a favorable process with a reaction energy of −7.92 kcal mol^{-1} and an activation energy of 40.1 kcal mol^{-1}. The activation energies for the remaining species from Scheme 7 are 36.9, 40.2, and 39.3 kcal mol^{-1} for formation of HEA, HHEA, and BHEOX, respectively.

Our final consideration was the formation of 4-(2-hydroxyethyl)piperazinone (HEPO). This has been observed to form in pilot plants as a mixture of two isomers, one major and one minor—dependent on the positioning of the carbonyl group. It has been theorized to form via a ring closing reaction from *N*-(2-hydroxyethyl)−2-(2-hydroxyethylamino)acetamide (HEHEAA), as shown in Scheme 8. Either of the internal nitrogen atoms can act as a nucleophile and react with a carbon five bonds away to yield the product. The resulting energy profile is shown in Figure 17.

The stabilities of the major and minor products are very similar. In contrast, the transition state leading to the major product species is 17 kcal mol^{-1} lower in energy than that leading to the minor species. The relatively high activation energies is consistent with experimental observations that suggest that prolonged exposure to high temperatures is needed to observe the formation of HEPO.[3]

3.6. Schematic Reaction Network. The above computational investigations have presented possible chemical pathways leading to the formation of likely degradation products of MEA. Table 1 summarizes these reactions along with activation parameters, reaction energies, and Arrhenius factors. These reactions can provide the basis for the construction of a full chemical kinetic mechanism that can predict and control the rate of thermal degradation in experimental plants. This will form the basis of a future publication.

4. CONCLUSIONS

In this work, we have reported on the DFT calculations of various important reactions involved in both the thermal and oxidative degradation of monoethanolamine. Activation and reaction energies were calculated and evaluated to rationalize which chemical pathways are most favored.

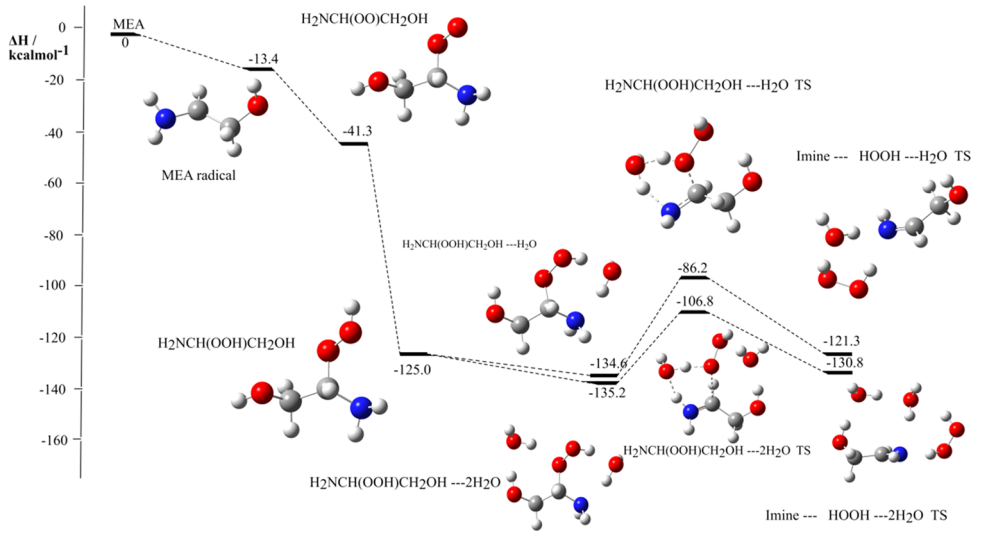

Figure 15. DFT-calculated ΔH energy profile for the formation of HOOH and an imine from MEA, highlighting the difference between one and two explicit water molecules.

https://dx.doi.org/10.1021/acs.iecr.0c03003
Ind. Eng. Chem. Res. XXXX, XXX, XXX−XXX

Scheme 7. Amide Formation from Reaction of MEA and Various Organic Acids

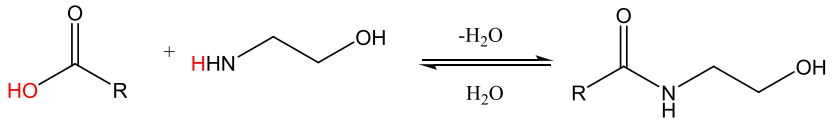

R = H	HEF
R = Me	HEA
R = CH_2OH	HHEA
R = $C(O)NHCH_2CH_2OH$	BHEOX

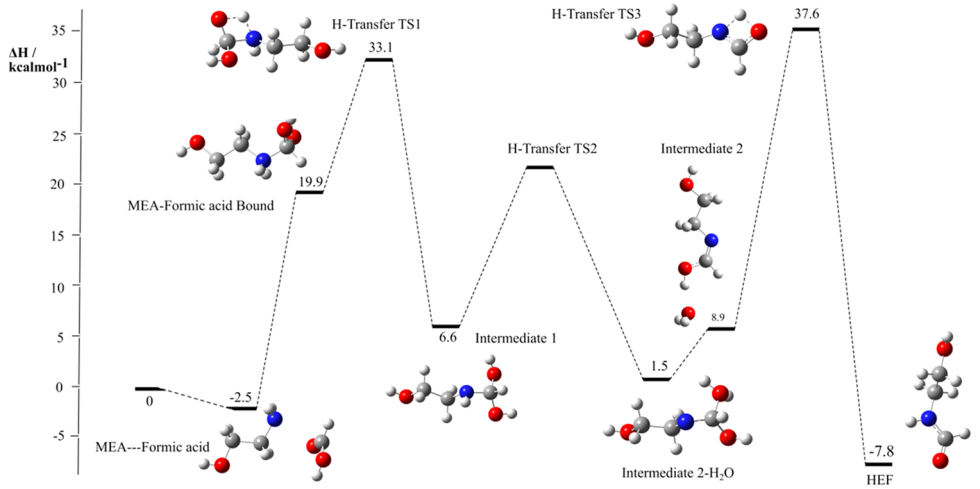

Figure 16. DFT-calculated ΔH energy profile for the formation of HEF from MEA and formic acid.

Scheme 8. Proposed Mechanism for HEPO Formation from HEHEAA[a]

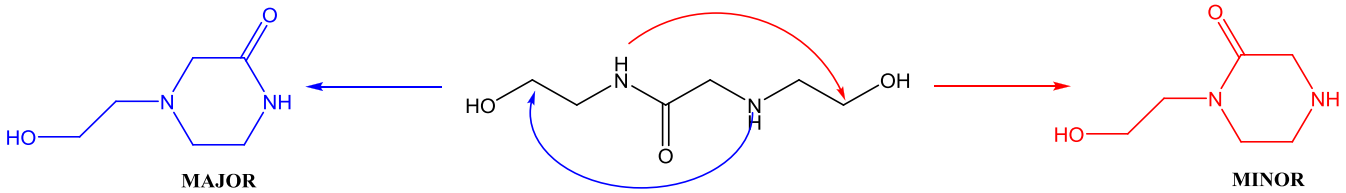

[a]Red: Minor Product. Blue: Major Product.

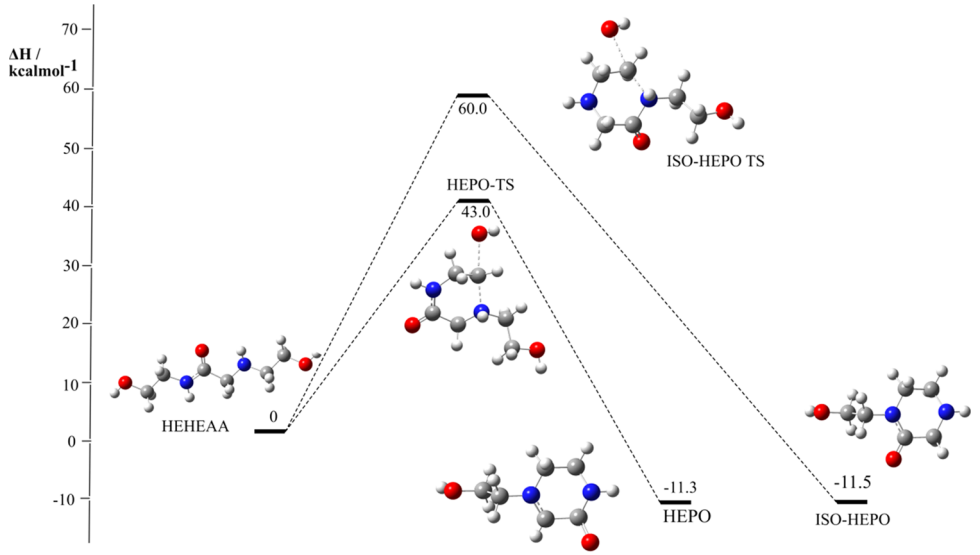

Figure 17. DFT-calculated ΔH energy profile for the formation of two isomers of HEPO from HEHEAA.

https://dx.doi.org/10.1021/acs.iecr.0c03003
Ind. Eng. Chem. Res. XXXX, XXX, XXX−XXX

Table 1. Summarized Reactions Detailing the Formation of Common Degradation Products of Thermal and Oxidative Degradation of MEA and Associated Activation Energies, Reaction Energies, and Arrhenius Parameters

reaction	E_a (kcal mol^{-1})	reaction energy(kcal mol^{-1})	A
$MEACO_2$ → carbamic acid	22.9	−8.9	1.99×10^{13}
$MEACO_2$ + MEA → ion pair	15.4	−27.2	2.28×10^{11}
ion pair → OZD + MEA + H_2O	39.5	6.3	1.65×10^{13}
carbamic acid + H_2O → isocyanate + $2H_2O$	34.8	4.5	9.64×10^{10}
isocyanate + MEA → BHEU	28.8	−23.6	1.33×10^{10}
isocyanate + MEA + $MEAH^+$ → OZD + MEA + $MEAH^+$	2.9	−35.3	2.20×10^{9}
OZD + MEA → HEEDA + CO_2	27.3	0.2	4.49×10^{10}
HEEDA + CO_2 → HEIA + H_2O	36.5	−6.7	9.64×10^{7}
HEEDA + OZD → AHEIA + H_2O	33.7	−10.9	3.91×10^{12}
MEA + $R^{\bullet}$ → RH + MEA radical	9.6	−13.4	1.86×10^{11}
MEA radical + O_2 + "$H^{\bullet}$" → MEA − OOH	0.0	−125.0	
MEA − OOH → Imine + HOOH	28.7	4.4	4.84×10^{11}
MEA + formic acid → HEF	40.1	−7.9	3.76×10^{11}
MEA + ethanoic acid → HEA	36.9	−5.0	2.74×10^{11}
MEA + 2 − OH − ethanoic acid → HHEA	40.2	−6.6	3.89×10^{11}
MEA + 2 − R − ethanoic acid → BHEOX	39.3	−12.3	5.72×10^{11}
HEHEAA → HEPO	43.0	−11.3	9.64×10^{9}

Carbamate, formed via the reaction of MEA with CO_2, preferentially forms an ion pair with a further molecule of MEA over internal H-transfer to form carbamic acid. However, the formation of carbamic acid may become important at higher loadings of CO_2, which would reduce the available MEA in the system. Carbamic acid can dehydrate to form isocyanate, which subsequently can react with MEA to form BHEU, a related compound to UREA. Furthermore, isocyanate can cyclize to form OZD.

OZD reacts favorably to form HEEDA via a ring opening reaction with MEA. HEEDA can cyclize to form HEIA or react with MEA to form AHEIA. Both reactions are thermodynamically favorable and kinetically viable given the operating conditions in amine plants.

Potential mechanistic pathways to the formation of major degradation products of MEA have been established. Using the associated activation energies and Arrhenius data, it might be possible to propose new amine species, which are more resistant to degradation via the utilization of a full chemical kinetic mechanism.

■ ASSOCIATED CONTENT

Supporting Information

The Supporting Information is available free of charge at https://pubs.acs.org/doi/10.1021/acs.iecr.0c03003.

Cartesian coordinates for DFT-optimized structures. Equivalent data to that found in the main text using M06 functional, Def2-TZVP basis set, and SMD solvent model (PDF)

■ AUTHOR INFORMATION

Corresponding Author

Christopher Parks − *Department of Mechanical Engineering, The University of Sheffield, Sheffield S3 7RD, U.K.;* orcid.org/0000-0001-8016-474X; Email: c.m.parks@sheffield.ac.uk

Authors

Ehsan Alborzi − *Department of Mechanical Engineering, The University of Sheffield, Sheffield S3 7RD, U.K.;* orcid.org/0000-0002-2585-0824

Muhammad Akram − *Department of Mechanical Engineering, The University of Sheffield, Sheffield S3 7RD, U.K.*

Mohammed Pourkashanian − *Department of Mechanical Engineering, The University of Sheffield, Sheffield S3 7RD, U.K.*

Complete contact information is available at: https://pubs.acs.org/10.1021/acs.iecr.0c03003

Notes

The authors declare no competing financial interest.

■ REFERENCES

(1) UNFCCC. Adoption of the Paris Agreement. Report No. FCCC/CP/2015/L.9/Rev.1; 2015. http://unfccc.int/resource/docs/2015/cop21/eng/l09r01.pdf.

(2) Seinfeld, J. H. Insights on global warming. *AIChE J.* **2011**, *57*, 3259−3284.

(3) da Silva, E. F.; Lepaumier, H.; Grimstvedt, A.; Vevelstad, S. J.; Einbu, A.; Vernstad, K.; Svendsen, H. F.; Zahlsen, K. Understanding 2-Ethanolamine Degradation in Postcombustion CO2 Capture. *Ind. Eng. Chem. Res.* **2012**, *51*, 13329−13338.

(4) Goff, G. S.; Rochelle, G. T. Oxidation Inhibitors for Copper and Iron Catalyzed Degradation of Monoethanolamine in CO2 Capture Processes. *Ind. Eng. Chem. Res.* **2006**, *45*, 2513−2521.

(5) Rao, A. B.; Rubin, E. S. A Technical, Economic, and Environmental Assessment of Amine-Based CO2 Capture Technology for Power Plant Greenhouse Gas Control. *Environ. Sci. Technol.* **2002**, *36*, 4467−4475.

(6) Reynolds, A. J.; Verheyen, T. V.; Adeloju, S. B.; Meuleman, E.; Feron, P. Towards Commercial Scale Postcombustion Capture of CO2 with Monoethanolamine Solvent: Key Considerations for Solvent Management and Environmental Impacts. *Environ. Sci. Technol.* **2012**, *46*, 3643−3654.

(7) Polderman, L. D.; Dillon, C. P.; Steele, A. B. Why monoethanolamine solution breaks down in gas-treating service. *Oil Gas J.* **1955**, *54*, 180−183.

(8) Kohl, A. L.; Nielsen, R. B. *Gas Purification*, 5th ed.; Elsevier: Houston, TX, 1997; pp 278−329.

https://dx.doi.org/10.1021/acs.iecr.0c03003
Ind. Eng. Chem. Res. XXXX, XXX, XXX−XXX

(9) Davis, J.; Rochelle, G. Thermal degradation of monoethanolamine at stripper conditions. *Energy Procedia* **2009**, *1*, 327−333.
(10) Kim, C. J.; Sartori, G. Kinetics and mechanism of diethanolamine degradation in aqueous solutions containing carbon dioxide. *Int. J. Chem. Kinet.* **1984**, *16*, 1257−1266.
(11) Chi, S.; Rochelle, G. T. Oxidative Degradation of Monoethanolamine. *Ind. Eng. Chem. Res.* **2002**, *41*, 4178−4186.
(12) Goff, G. S.; Rochelle, G. T. Monoethanolamine Degradation: O2 Mass Transfer Effects under CO2 Capture Conditions. *Ind. Eng. Chem. Res.* **2004**, *43*, 6400−6408.
(13) Vevelstad, S. J.; Eide-Haugmo, I.; da Silva, E. F.; Svendsen, H. F. Degradation of MEA; a theoretical study. *Energy Procedia* **2011**, *4*, 1608−1615.
(14) Saeed, I. M.; Lee, V. S.; Mazari, S. A.; Si Ali, B.; Basirun, W. J.; Asghar, A.; Ghalib, L.; Jan, B. M. Thermal degradation of aqueous 2-aminoethylethanolamine in CO_2 capture; identification of degradation products, reaction mechanisms and computational studies. *Chem. Cent. J.* **2017**, *11*, No. 10.
(15) Yoon, B.; Stowe, H. M.; Hwang, G. S. Molecular mechanisms for thermal degradation of CO2-loaded aqueous monoethanolamine solution: a first-principles study. *Phys. Chem. Chem. Phys.* **2019**, *21*, 22132−22139.
(16) Davran-Candan, T. DFT Modeling of CO2 Interaction with Various Aqueous Amine Structures. *J. Phys. Chem. A* **2014**, *118*, 4582−4590.
(17) Matsuzaki, Y.; Yamada, H.; Chowdhury, F. A.; Higashii, T.; Onoda, M. Ab Initio Study of CO2 Capture Mechanisms in Aqueous Monoethanolamine: Reaction Pathways for the Direct Interconversion of Carbamate and Bicarbonate. *J. Phys. Chem. A* **2013**, *117*, 9274−9281.
(18) Yamada, H.; Matsuzaki, Y.; Higashii, T.; Kazama, S. Density Functional Theory Study on Carbon Dioxide Absorption into Aqueous Solutions of 2-Amino-2-methyl-1-propanol Using a Continuum Solvation Model. *J. Phys. Chem. A* **2011**, *115*, 3079−3086.
(19) Yang, X.; Rees, R. J.; Conway, W.; Puxty, G.; Yang, Q.; Winkler, D. A. Computational Modeling and Simulation of CO2 Capture by Aqueous Amines. *Chem. Rev.* **2017**, *117*, 9524−9593.
(20) Frisch, M. J.; Trucks, G. W.; Schlegel, H. B.; Scuseria, G. E.; Robb, M. A.; Cheeseman, J. R.; Scalmani, G.; Barone, V.; Mennucci, B.; Petersson, G. A.; Nakatsuji, H.; Caricato, M.; Li, X.; Hratchian, H. P.; Izmaylov, A. F.; Bloino, J.; Zheng, G.; Sonnenberg, J. L.; Hada, M.; Ehara, M.; Toyota, K.; Fukuda, R.; Hasegawa, J.; Ishida, M.; Nakajima, T.; Honda, Y.; Kitao, O.; Nakai, H.; Vreven, T.; J. A. Montgomery, J.; Peralta, J. E.; Ogliaro, F.; Bearpark, M.; Heyd, J. J.; Brothers, E.; Kudin, K. N.; Staroverov, V. N.; Keith, T.; Kobayashi, R.; Normand, J.; Raghavachari, K.; Rendell, A.; Burant, J. C.; Iyengar, S. S.; Tomasi, J.; Cossi, M.; Rega, N.; Millam, J. M.; Klene, M.; Knox, J. E.; Cross, J. B.; Bakken, V.; Adamo, C.; Jaramillo, J.; Gomperts, R.; Stratmann, R. E.; Yazyev, O.; Austin, A. J.; Cammi, R.; C. Pomelli, J. W. O.; Martin, R. L.; Morokuma, K.; Zakrzewski, V. G.; Voth, G. A.; Salvador, P.; Dannenberg, J. J.; Dapprich, S.; Daniels, A. D.; Farkas, O.; Foresman, J. B.; Ortiz, J. V.; Cioslowski, J.; Fox, D. J.. *Gaussian 09*, 2016.
(21) Becke, A. D. Density-functional exchange-energy approximation with correct asymptotic behavior. *Phys. Rev. A* **1988**, *38*, 3098−3100.
(22) Lee, C.; Yang, W.; Parr, R. G. Development of the Colle-Salvetti correlation-energy formula into a functional of the electron density. *Phys. Rev. B* **1988**, *37*, 785−789.
(23) Perdew, J. P.; Chevary, J. A.; Vosko, S. H.; Jackson, K. A.; Pederson, M. R.; Singh, D. J.; Fiolhais, C. Atoms, molecules, solids, and surfaces: Applications of the generalized gradient approximation for exchange and correlation. *Phys. Rev. B* **1992**, *46*, 6671−6687.
(24) Dunning, T. H., Jr. Gaussian basis sets for use in correlated molecular calculations. I. The atoms boron through neon and hydrogen. *J. Chem. Phys.* **1989**, *90*, 1007−1023.
(25) Stowe, H. M.; Vilčiauskas, L.; Paek, E.; Hwang, G. S. On the origin of preferred bicarbonate production from carbon dioxide (CO2) capture in aqueous 2-amino-2-methyl-1-propanol (AMP). *Phys. Chem. Chem. Phys.* **2015**, *17*, 29184−29192.
(26) Hwang, G. S.; Stowe, H. M.; Paek, E.; Manogaran, D. Reaction mechanisms of aqueous monoethanolamine with carbon dioxide: a combined quantum chemical and molecular dynamics study. *Phys. Chem. Chem. Phys.* **2015**, *17*, 831−839.
(27) Zhao, Y.; Truhlar, D. G. The M06 suite of density functionals for main group thermochemistry, thermochemical kinetics, noncovalent interactions, excited states, and transition elements: two new functionals and systematic testing of four M06-class functionals and 12 other functionals. *Theor. Chem. Acc.* **2008**, *120*, 215−241.
(28) Scalmani, G.; Frisch, M. J. Continuous surface charge polarizable continuum models of solvation. I. General formalism. *J. Chem. Phys.* **2010**, *132*, No. 114110.
(29) Cossi, M.; Barone, V. Analytical second derivatives of the free energy in solution by polarizable continuum models. *J. Chem. Phys.* **1998**, *109*, 6246−6254.
(30) Marenich, A. V.; Cramer, C. J.; Truhlar, D. G. Universal Solvation Model Based on Solute Electron Density and on a Continuum Model of the Solvent Defined by the Bulk Dielectric Constant and Atomic Surface Tensions. *J. Phys. Chem. B* **2009**, *113*, 6378−6396.
(31) Grimme, S.; Ehrlich, S.; Goerigk, L. Effect of the damping function in dispersion corrected density functional theory. *J. Comput. Chem.* **2011**, *32*, 1456−1465.
(32) Cancès, E.; Mennucci, B.; Tomasi, J. A new integral equation formalism for the polarizable continuum model: Theoretical background and applications to isotropic and anisotropic dielectrics. *J. Chem. Phys.* **1997**, *107*, 3032−3041.
(33) Funes-Ardoiz, I.; Paton, R. S.. *GoodVibes*. Version 2.0.3; Zenodo, 2018.
(34) Stowe, H. M.; Hwang, G. S. Fundamental Understanding of CO2 Capture and Regeneration in Aqueous Amines from First-Principles Studies: Recent Progress and Remaining Challenges. *Ind. Eng. Chem. Res.* **2017**, *56*, 6887−6899.
(35) Matin, N. S.; Thompson, J.; Onneweer, F. M.; Liu, K. Thermal Degradation Rate of 2-Amino-2-methyl-1-propanol to Cyclic 4,4-Dimethyl-1,3-oxazolidin-2-one; Mechanistic Aspects and Kinetics Investigation. *Ind. Eng. Chem. Res.* **2017**, *56*, 9437−9445.
(36) Heldebrant, D. J.; Koech, P. K.; Glezakou, V.-A.; Rousseau, R.; Malhotra, D.; Cantu, D. C. Water-Lean Solvents for Post-Combustion CO2 Capture: Fundamentals, Uncertainties, Opportunities, and Outlook. *Chem. Rev.* **2017**, *117*, 9594−9624.
(37) Yamada, H. Comparison of Solvation Effects on CO2 Capture with Aqueous Amine Solutions and Amine-Functionalized Ionic Liquids. *J. Phys. Chem. B* **2016**, *120*, 10563−10568.
(38) Shaikh, A. R.; Karkhanechi, H.; Kamio, E.; Yoshioka, T.; Matsuyama, H. Quantum Mechanical and Molecular Dynamics Simulations of Dual-Amino-Acid Ionic Liquids for CO2 Capture. *J. Phys. Chem. C* **2016**, *120*, 27734−27745.
(39) Iida, K.; Yokogawa, D.; Ikeda, A.; Sato, H.; Sakaki, S. Carbon dioxide capture at the molecular level. *Phys. Chem. Chem. Phys.* **2009**, *11*, 8556−8559.
(40) Arstad, B.; Blom, R.; Swang, O. CO2 Absorption in Aqueous Solutions of Alkanolamines: Mechanistic Insight from Quantum Chemical Calculations. *J. Phys. Chem. A* **2007**, *111*, 1222−1228.
(41) Xie, H.-B.; Zhou, Y.; Zhang, Y.; Johnson, J. K. Reaction Mechanism of Monoethanolamine with CO2 in Aqueous Solution from Molecular Modeling. *J. Phys. Chem. A* **2010**, *114*, 11844−11852.
(42) Peterson, S. L.; Stucka, S. M.; Dinsmore, C. J. Parallel Synthesis of Ureas and Carbamates from Amines and CO2 under Mild Conditions. *Org. Lett.* **2010**, *12*, 1340−1343.
(43) Sakakura, T.; Choi, J.-C.; Yasuda, H. Transformation of Carbon Dioxide. *Chem. Rev.* **2007**, *107*, 2365−2387.
(44) Lepaumier, H.; da Silva, E. F.; Einbu, A.; Grimstvedt, A.; Knudsen, J. N.; Zahlsen, K.; Svendsen, H. F. Comparison of MEA degradation in pilot-scale with lab-scale experiments. *Energy Procedia* **2011**, *4*, 1652−1659.

https://dx.doi.org/10.1021/acs.iecr.0c03003
Ind. Eng. Chem. Res. XXXX, XXX, XXX−XXX

(45) Fazio, M. J. Nucleophilic ring opening of 2-oxazolines with amines: a convenient synthesis for unsymmetrically substituted ethylenediamines. *J. Org. Chem.* **1984**, *49*, 4889−4893.
(46) Gouedard, C.; Picq, D.; Launay, F.; Carrette, P. L. Amine degradation in CO2 capture. I. A review. *Int. J. Greenhouse Gas Control* **2012**, *10*, 244−270.
(47) Lepaumier, H.; Picq, D.; Carrette, P.-L. New Amines for CO2 Capture. II. Oxidative Degradation Mechanisms. *Ind. Eng. Chem. Res.* **2009**, *48*, 9068−9075.
(48) Fredriksen, S. B.; Jens, K.-J. Oxidative Degradation of Aqueous Amine Solutions of MEA, AMP, MDEA, Pz: A Review. *Energy Procedia* **2013**, *37*, 1770−1777.
(49) Koppenol, W. H.; Stanbury, D. M.; Bounds, P. L. Electrode potentials of partially reduced oxygen species, from dioxygen to water. *Free Radical Biol. Med.* **2010**, *49*, 317−322.
(50) Wood, P. M. The potential diagram for oxygen at pH 7. *Biochem. J.* **1988**, *253*, 287−289.
(51) Supap, T.; Idem, R.; Tontiwachwuthikul, P.; Saiwan, C. Analysis of Monoethanolamine and Its Oxidative Degradation Products during CO2 Absorption from Flue Gases: A Comparative Study of GC-MS, HPLC-RID, and CE-DAD Analytical Techniques and Possible Optimum Combinations. *Ind. Eng. Chem. Res.* **2006**, *45*, 2437−2451.
(52) Vevelstad, S. J.; Grimstvedt, A.; Elnan, J.; da Silva, E. F.; Svendsen, H. F. Oxidative degradation of 2-ethanolamine: The effect of oxygen concentration and temperature on product formation. *Int. J. Greenhouse Gas Control* **2013**, *18*, 88−100.

https://dx.doi.org/10.1021/acs.iecr.0c03003
Ind. Eng. Chem. Res. XXXX, XXX, XXX−XXX